Advances in Computational Design, *Vol. 6, No. 3 (2021) 169-190*
https://doi.org/10.12989/acd.2021.6.3.169

Mechanical behavior of RC cantilever beams strengthened with FRP laminate plate

Rabahi Abderezak[1,2], Hassaine Daouadji Tahar*[1], Benferhat Rabia[1,2] and Abdelouahed Tounsi[3,4,5]

[1]Civil Engineering Department, University of Tiaret, Algeria
[2]Laboratory of Geomatics and Sustainable Development, University of Tiaret, Algeria
[3]YFL (Yonsei Frontier Lab), Yonsei University, Seoul, Korea
[4]Department of Civil and Environmental Engineering, King Fahd University of Petroleum & Minerals, 31261 Dhahran, Saudi Arabia.
[5]LMH Laboratory, Civil Engineering Department, University of Sidi Bel Abbes, Algeria

(Received June 10, 2020, Revised May 21, 2021, Accepted June 3, 2021)

Abstract. In this paper, an analytical interfacial stress analysis is presented for simply supported concrete cantilever beam bonded with a composite plate. The adherend shear deformations have been included in the present analyses by assuming a linear shear stress through the thickness of the adherends, one of the strong points of this model; this shear parameter has not been taken up by other researchers. Remarkable effect of shear deformations of adherends has been noted in the results. Indeed, the resulting interfacial stresses concentrations are considerably smaller than those obtained by other models which neglect adherent shear deformations. It is shown that both the normal and shear stresses at the interface are influenced by the material and geometry parameters of the composite beam. The theoretical predictions are compared with other existing solutions. This type of research is very useful for structural calculating engineers who are always looking to optimize strengthening design parameters and implement reliable debonding prevention measures.

Keywords: composite plate; interfacial stresses; RC cantilever beam; strengthening

1. Introduction

Advanced composite materials have been used successfully for repairing reinforced concrete structures for a number of years (Tounsi 2006, Smith and Teng 2002). In structural science calculations, composite plates have mainly been used to rehabilitate concrete structure, significant interesting in recent years. The main advantages of composite materials are their high strength-to-weight ratio and their excellent resistance against corrosion and chemical attacks. An important topic arising in the study of plated RC cantilever beams is the evaluation of interactions at RC–composite interface. These interactions, in fact, permit the transmission of stresses from the core to the plate composite; if they go over a limit value the premature failure of the strengthened beam

*Corresponding author, M.Sc., E-mail: daouadjitah@yahoo.fr

http://www.techno-press.org/?journal=acd&subpage=7 ISSN: 2383-8477 (Print), 2466-0523 (Online)

can occur.

Several closed-form solutions have been developed in the past decade for the interfacial stresses in beams bonded with a composite plate (Ashraful *et al*. 2018, AlSaid-Alwan *et al*. 2020, Yaylaci *et al*. 2020, Zenzen *et al*. 2020, Bendada *et al*. 2020, Fethi *et al*. 2019, Belaid *et al*. 2019, Benferhat *et al*. 2018, Bensattalah *et al*. 2018, Daouadji 2013, Adim *et al*. 2016b, Belkacem *et al*. 2016a, Benferhat *et al*. 2020, Rabia *et al*. 2020, Guenaneche *et al*. 2014, Krour *et al*. 2014, Liu *et al*. 2019, Panjehpour *et al*. 2014, Chaded *et al*. 2018, Rabahi *et al*. 2018, Rabia *et al*. 2016, El Mahi *et al*. 2014, Panjehpour *et al*. 2016, Pello *et al*. 2020, Rabahi *et al*. 2019, Yu-Hang *et al*. 2020, Yang *et al*. 2007, Yuan *et al*. 2019). All these solutions are for linear elastic materials and employ the same key assumption that the adhesive is subject to normal and shear stresses that are constant across the thickness of the adhesive layer. It is this key assumption that enables relatively simple closed-form solutions to be obtained. In the existing solutions, two different approaches have been employed. some researchers who have used a staged analysis approach, while other researchers such as (Abdelhak *et al*. 2016, Bekki *et al*. 2021, Benferhat *et al*. 2021a, Rabahi *et al*. 2021b, Daouadji *et al*. 2021, Abdedezak *et al*. 2018, Benhenni *et al*. 2019, Adim *et al*. 2018, Benyoucef *et al*. 2007, Smith and Teng 2002, Tounsi *et al*. 2008, Bensatallah *et al*.2020, Tlidji *et al*.2021, Bekki *et al*. 2019, Chergui *et al*. 2019, Hamrat *et al*. 2020, Adim *et al*. 2016a, Belkacem *et al*. 2016b, Benferhat, *et al*. 2016, Benhenni *et al*. 2018, Bensattalah *et al*. 2020, Hassaine *et al*. 2019, Hassaine *et al*.2008, Hassaine *et al*. 2016b, Rabahi *et al*. 2016, Rabia *et al*. 2019, Kablia *et al*.2020 Rabahi *et al*. 2020, Hassaine Daouadji *et al*. 2020, Benferhat *et al*. 2021b, Abdelhak *et al*. 2021, Rabahi *et al*. 2021a Hassaine Daouadji 2017 and Benferhat *et al*. (2019), considered directly deformation compatibility conditions. It is the latter that is adopted as an approach in this study of the behaviour of composite-strengthened RC cantilever beam.

The objectives of this paper are first to present an improvement to Hassaine (2016a) solution to obtain a new closed-form solution which accounts for the parabolic adherend shear deformation effect in both the RC cantilever beam and bonded plate and second to compare quantitatively its solution against the new one developed in this paper by numerical illustrations. Numerical applications and a parametric study are presented to illustrate the governing parameters that control the stress concentrations at the edge of the composite strip. Finally, the adopted improved model describes better the actual response of the composite- RC hybrid cantilever beams and permits the evaluation of the adhesive stresses, the knowledge of which is very important in the design of such structures. The adopted model describes better the actual response of the composite- RC hybrid cantilever beam and permits the evaluation of the interfacial stresses, the knowledge of which is very important in the design of such structures.

2. Theoretical analysis and solutions procedure

2.1 Research significance

The most common failure modes for composite strengthened RC cantilever beams are debonding of the composite plate or ripping of the concrete cover. These types of failures prevent the strengthened cantilever beam for reaching its ultimate flexural capacity, and therefore they must be included in design considerations. Both of these premature failure modes are caused by shear and normal stress concentrations in adhesive layer. In this paper, an improved theoretical interfacial stress analysis is presented for RC cantilever beams strengthened with FRP laminate

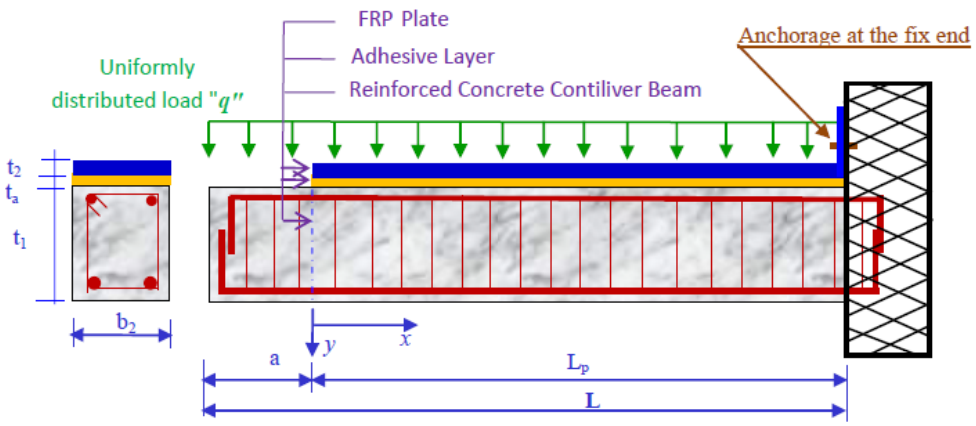

Fig. 1 RC cantilever member strengthening with composite plate

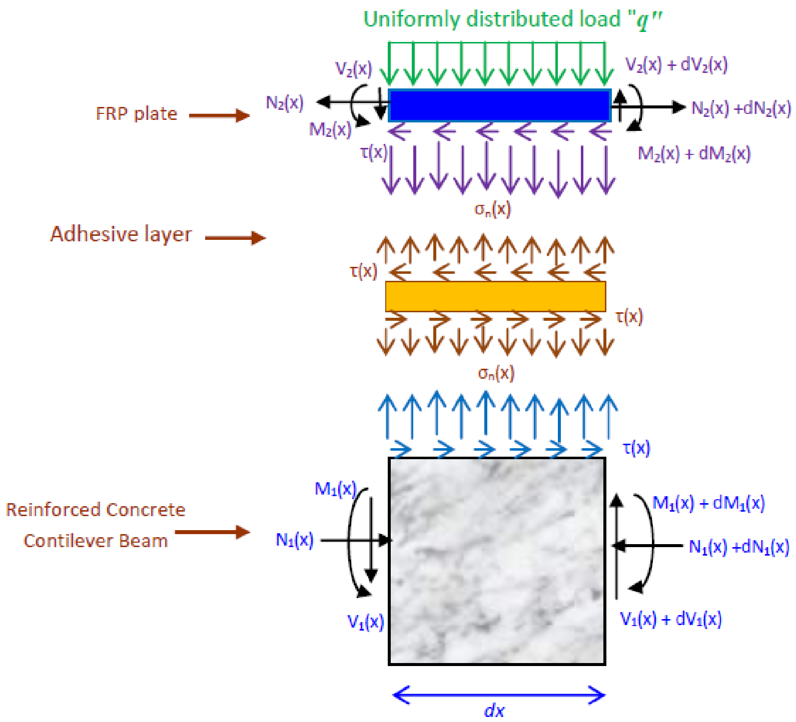

Fig. 2 Forces in an infinitesimal element of an FRP-strengthened RC cantilever member

plate. Where the adherend shear deformations have been included in the present theoretical analyses by assuming a linear shear stress through the thickness of the adherends, while all existing solutions neglect this effect. In this context closed form solutions of stress concentrations are required in developing design guidelines for strengthening reinforced concrete cantilever beams with composite plates.

2.2 Theoretical formulation

Basic assumptions: To simplify the theoretical derivations of interfacial stresses in FRP-strengthened cantilever members (Fig. 1), the following assumptions are adopted in this article.

- The composite materials, including concrete, adhesive layer and FRP laminates, are all linear elastic.
- The average cross-sectional strain in bending conforms to the plane-section assumption before and after strengthening.
- There is no slip at the FRP to adhesive inter-face or at the adhesive to concrete interface before debonding failure.
- The shear and normal stresses in the adhesive layer are constant through the thickness, and the in plane bending stiffness of the adhesive layer is neglected.
- In the derivation of interfacial shear stress, the moment curvatures of both the cantilever member and the externally bonded FRP laminates are equal.

In the present analysis, a linear elastic behavior is assumed for the three materials (concrete, adhesive and composite plate). The adhesive layer is supposed to play a role in transferring the stresses from the concrete to the composite plate with constant stresses throughout its thickness (Fig. 2).

Elasticity equations: The deformation in concrete in the vicinity of the adhesive layer can be expressed by (Fig. 2):

$$\varepsilon_1(x) = \frac{du_1(x)}{dx} = \varepsilon_1^M(x) + \varepsilon_1^N(x) \tag{1a}$$

with

$$\varepsilon_1^M(x) = \frac{y_1}{E_1 I_1} M_1(x) \quad \text{and} \quad \varepsilon_1^N(x) = \frac{du_1^N(x)}{dx} = \frac{N_1}{E_1 A_1} \tag{1b}$$

$$\varepsilon_1(x) = \frac{du_1(x)}{dx} = \frac{y_1}{E_1 I_1} M_1(x) + \frac{N_1}{E_1 A_1} \tag{1c}$$

Based on the theory of laminated sheets, the deformation of the composite sheet in the vicinity of the adhesive layer is given by:

$$\varepsilon_2(x) = \frac{du_2(x)}{dx} = \varepsilon_2^M(x) + \varepsilon_2^N(x) \tag{2a}$$

with

$$\varepsilon_2^M(x) = \frac{-y_2}{E_2 I_2} M_2(x) \quad \text{and} \quad \varepsilon_2^N(x) = \frac{du_2^N(x)}{dx} = A_{11}' \frac{N_2(x)}{b_2} \tag{2b}$$

$$\varepsilon_2(x) = \frac{du_2(x)}{dx} = -D_{11}' \frac{y_2}{b_2} M_2(x) + A_{11}' \frac{N_2(x)}{b_2} \tag{2c}$$

Where $u_1(x)$ and $u_2(x)$ are the horizontal displacements of the concrete beam and the composite plate respectively. $M_1(x)$ and $M_2(x)$ are respectively the bending moments applied to the concrete beam and the composite plate; E_1 is the Young's modulus of concrete; I_1 the moment of inertia, N_1 and N_2 are the axial forces applied to the concrete and the composite plate respectively, b_1 and t_1 are the width and thickness of the reinforcement plate, $[A']=[A^{-1}]$ is the inverse of the membrane matrix $[A]$, $[D']=[D^1]$ is the inverse of the bending matrix

By writing the conditions of equilibrium of the member 1 (concrete), we will have:

In the X direction:

$$\frac{dN_1(x)}{dx} = -b_1\tau(x) \tag{3a}$$

Where $\tau(x)$ is the shear stress in the adhesive layer.

In the y direction:

$$\frac{dV_1(x)}{dx} = -(\sigma_n(x)b_1 + qb_1) \tag{3b}$$

Where $V_1(x)$ the sheer force of the concrete beam is, $\sigma(x)$ is the normal stress at the adhesive layer, q is the distributed load and b_1 the width of the concrete beam.

The moment of balance:

$$\frac{dM_1(x)}{dx} = V_1(x) - b_1 y_1 \tau(x) \tag{4}$$

The balance of the FRP reinforcement plate in the x and y directions, as well as the moment of equilibrium are written as follows:

In the x direction:

$$\frac{dN_2(x)}{dx} = b_2\tau(x) \tag{5a}$$

In the y direction:

$$\frac{dV_2(x)}{dx} = \sigma_n(x)b_2 \tag{5b}$$

The moment of balance:

$$\frac{dM_2(x)}{dx} = V_2(x) - b_2 y_2 \tau(x) \tag{5c}$$

Where $V_2(x)$ is the shear force of the reinforcement plate.

In what follows, the stiffness of the reinforcement plate is significantly lower than that of the concrete beam to be reinforced. The bending moment in the composite plate can be neglected to simplify the shear stress derivation operations.

On the other hand, the laminate theory is used to determine the stress and strain of the externally bonded composite plate in order to investigate the whole mechanical performance of the composite strengthened structure. The effective modules of the composite laminate are varied by the orientation of the fibre directions and arrangements of the laminate patterns. The classical laminate theory is used to estimate the strain of the composite plate, i.e.,

$$\begin{Bmatrix} \varepsilon^0 \\ k \end{Bmatrix} = \begin{bmatrix} A' & B' \\ C' & D' \end{bmatrix} \begin{Bmatrix} N \\ M \end{Bmatrix} \tag{6}$$

$$\begin{aligned} [A'] &= [A]^{-1} + [A]^{-1}[B][D^*]^{-1}[B][A]^{-1} \\ [B'] &= -[A]^{-1}[B][D^*]^{-1} \\ [C'] &= [B']^T \\ [D'] &= [D^*]^{-1} \\ [D^*] &= [D] - [B][A]^{-1}[B] \end{aligned} \tag{7}$$

The terms of the matrices $[A]$, $[B]$ and $[D]$ are written as:
Extensional matrix:

$$A_{ij} = \sum_{k=1}^{NN} \overline{Q}_{ij}^{k} ((y_2)_k - (y_2)_{k-1}) \tag{8}$$

Extensional – bending coupled matrix:

$$B_{ij} = \frac{1}{2} \sum_{k=1}^{NN} \overline{Q}_{ij}^{k} ((y_2^2)_k - (y_2^2)_{k-1}) \tag{9}$$

Flexural matrix:

$$D_{ij} = \frac{1}{3} \sum_{k=1}^{NN} \overline{Q}_{ij}^{k} ((y_2^3)_k - (y_2^3)_{k-1}) \tag{10}$$

The subscript *NN* represents the number of laminate layers of the FRP plate, $\overline{Q}_{ij}$ can be estimated by using the off-axis orthotropic plate theory, where:

$$\overline{Q}_{11} = Q_{11} m^4 + 2(Q_{12} + 2Q_{33}) m^2 n^2 + Q_{22} n^4 \tag{11a}$$

$$\overline{Q}_{12} = (Q_{11} + Q_{22} - 4Q_{33}) m^2 n^2 + Q_{12}(n^4 + m^4) \tag{11b}$$

$$\overline{Q}_{22} = Q_{11} n^4 + 2(Q_{12} + 2Q_{33}) m^2 n^2 + Q_{22} m^4 \tag{11c}$$

$$\overline{Q}_{33} = (Q_{11} + Q_{22} - 2Q_{12} - 2Q_{33}) m^2 n^2 + Q_{33}(n^4 + m^4) \tag{11d}$$

And

$$Q_{11} = \frac{E_1}{1 - \upsilon_{12}\upsilon_{21}} \tag{12a}$$

$$Q_{22} = \frac{E_2}{1-\upsilon_{12}\upsilon_{21}} \tag{12b}$$

$$Q_{12} = \frac{\upsilon_{12} E_2}{1-\upsilon_{12}\upsilon_{21}} = \frac{\upsilon_{21} E_1}{1-\upsilon_{12}\upsilon_{21}} \tag{12c}$$

$$Q_{33} = G_{12} \tag{12d}$$

$$m = \cos(\theta_j) \qquad n = \sin(\theta_j) \tag{12e}$$

Where j is number of the layer; h, $\overline{Q}_{ij}$ and θ_j are respectively the thickness, the Hooke's elastic tensor and the fibers orientation of each layer.

Assume that the ply arrangement of the plate is symmetrical with respect to the mid-plane axis $y_2=0$. A great simplification in laminate analysis then occurs by assuming that the coupling matrix B is identically zero. Therefore Eqs. (6)-(10) can be simplified to the following matrix form for a plate with a width of b_2:

$$\{\varepsilon^0\} = [A']\{N\}_2 \quad \text{and} \quad \{k\} = [D']\{M\}_2 \tag{13}$$

Where

$$\{\varepsilon^0\}_2 = \begin{Bmatrix} \varepsilon_x^0 \\ \varepsilon_y^0 \\ \gamma_{xy}^0 \end{Bmatrix} \quad \text{and} \quad \{k\}_2 = \begin{Bmatrix} k_x \\ k_y \\ k_{xy} \end{Bmatrix} \tag{14}$$

$$\{N\}_2 = \begin{Bmatrix} N_x \\ N_y \\ N_{xy} \end{Bmatrix}_2 \quad \text{and} \quad \{M\}_2 = \begin{Bmatrix} M_x \\ M_y \\ M_{xy} \end{Bmatrix}_2 \tag{15}$$

In the present study, only an axial load N_x and the bending moment M_x in the beam's longitudinal axis are considered, i.e., $N_y=N_{xy}=0$ and $M_y=M_{xy}=0$. Therefore, Eqs. (14) and (15) can be simplified to:

$$\varepsilon_x^0 = \frac{A'_{11} N_x}{b_2} \quad \text{and} \quad k_x = \frac{D'_{11} M_x}{b_2} \tag{16}$$

Using CLT, the strain at the top of the FRP plate 2 is given as:

$$\varepsilon_2(x) = \varepsilon_x^0 - k_x \frac{t_2}{2} \tag{17}$$

Substituting Eq. (12b) in (12c) gives the following equation:

$$\varepsilon_2(x) = \frac{du_2(x)}{dx} = -D'_{11} \frac{t_2}{2b_2} M(x) + A'_{11} \frac{N_2(x)}{b_2} \tag{18}$$

Where: $N_2(x) = N_x$ and $M_2(x) = M_x$

The subscripts 1 and 2 denote adherends 1 and 2, respectively. M(x), N(x) and V(x) are the bending moment, axial and shear forces in each adherend.

2.3 Shear stress distribution along the FRP–concrete interface:

The shear stress at the adhesive layer can be expressed as follows:

$$\tau_a = \tau(x) = K_s \Delta u(x) = K_s \left[u_2(x) - u_1(x)\right] \tag{19}$$

Where K_s is the shear stiffness of the adhesive layer per unit length. From equation (19) we can deduce the expression of K_s which is given by:

$$K_s = \frac{\tau(x)}{\Delta u(x)} = \frac{\tau(x)}{\Delta u(x)/t_a} \frac{1}{t_a} = \frac{G_a}{t_a} \tag{20}$$

$\Delta u(x)$ is the displacement relative to the adhesive interface, G_a et t_a are the modulus and thickness of the adhesive layer, respectively.

By differentiating the Eqs. (19), (1) and (2) with respect to x, and neglecting the bending moment of the composite plate we will have:

$$\frac{d\tau(x)}{dx} = K_s \left[\frac{du_2(x)}{dx} - \frac{du_1(x)}{dx}\right] \tag{21a}$$

$$\frac{d\tau(x)}{dx} = K_s[[-D'_{11}\frac{y_2}{b_2}M_2(x) + A'_{11}\frac{N_2(x)}{b_2}] - [\frac{y_1}{E_1 I_1}M_1(x) + \frac{N_1}{E_1 A_1}]] \tag{21b}$$

Assuming that the curvatures in the member 1 and 2 are equal, the relationship between the moments in the two members can be written as follows:

$$M_1(x) = RM_2(x) \tag{22}$$

With

$$R = \frac{E_1 I_1 D'_{11}}{b_2} \tag{23}$$

The total moment of equilibrium of the differential element of Fig. 2 is given by:

$$M_T(x) = M_1(x) + M_2(x) + N(x)(y_1 + t_a + y_2) \tag{24a}$$

$$M_T(x) = M_1(x) + M_2(x) + N(x)(y_1 + t_a + \frac{t_2}{2}) \tag{24b}$$

$M_T(x)$ is the total moment and $N(x)$ is given by the following expression:

$$N(x) = N_2(x) = N_1(x) = b_2 \int_0^x \tau(x) \tag{25}$$

The bending moment of the reinforced beam expressed as a function of the total moment applied and the interface shear stresses is given by:

$$M_1(x) = \frac{R}{R+1}\left[M_T(x) - b_2\int_0^x \tau(x)(y_1 + t_a + \frac{t_2}{2})dx\right] \tag{26}$$

$$M_2(x) = \frac{1}{R+1}\left[M_T(x) - b_2\int_0^x \tau(x)(y_1 + t_a + \frac{t_2}{2})dx\right] \tag{27}$$

By deriving expressions (16) and (17) we will have:

$$\frac{dM_1(x)}{dx} = \frac{R}{R+1}\left[V_T(x) - b_2\tau(x)(y_1 + t_a + \frac{t_2}{2})\right] \tag{28}$$

$$\frac{dM_2(x)}{dx} = \frac{1}{R+1}\left[V_T(x) - b_2\tau(x)(y_1 + t_a + \frac{t_2}{2})\right] \tag{29}$$

By differentiating equation (31) we will have:

$$\frac{d^2\tau(x)}{dx^2} = K_s\left[\frac{A_{11}^{'}}{b_2}\frac{dN_2(x)}{dx} - D_{11}^{'}\frac{t_2}{2b_2}\frac{dM_2(x)}{dx} - \frac{y_1}{E_1 I_1}\frac{dM_1(x)}{dx} + \frac{1}{E_1 A_1}\frac{dN_1(x)}{dx}\right] \tag{30}$$

The substitution of shear force (Eqs. (28) and (29)) and normal force (Eq. (25)) in equation (30) allows us to obtain the differential equation of the shear interface stresses:

$$\frac{d^2\tau(x)}{dx^2} - K_s\left(A_{11}^{'} + \frac{b_2}{E_1 A_1} + \frac{(y_1 + \frac{t_2}{2})(y_1 + t_a + \frac{t_2}{2})}{E_1 I_1 D_{11}^{'} + b_2} b_2 D_{11}^{'}\right)\tau(x) + K_s\left(\frac{(y_1 + \frac{t_2}{2})}{E_1 I_1 D_{11}^{'} + b_2} D_{11}^{'}\right)V_T(x) = 0 \tag{31}$$

The solution to the differential equation (Eq. (31)) above is given by:

$$\tau(x) = \Delta_1 \cosh(\xi x) + \Delta_2 \sinh(\xi x) + \alpha_1 V_T(x) \tag{32}$$

With

$$\xi = \sqrt{K_s\left(A_{11}^{'} + \frac{b_2}{E_1 A_1} + \frac{(y_1 + \frac{t_2}{2})(y_1 + t_a + \frac{t_2}{2})}{E_1 I_1 D_{11}^{'} + b_2} b_2 D_{11}^{'}\right)} \tag{33}$$

$$\alpha_1 = \frac{K_s}{\xi^2}\left(\frac{(y_1 + \frac{t_2}{2})}{E_1 I_1 D_{11}^{'} + b_2} D_{11}^{'}\right) \tag{34a}$$

$$\alpha_1 = \frac{K_s}{\xi^2}\left(\frac{(y_1 + \frac{t_2}{2})}{E_1 I_1 D_{11}^{'} + b_2} D_{11}^{'}\right) \tag{34b}$$

Δ_1 and Δ_2 are constant coefficients determined from the boundary conditions. For our case of a uniformly distributed load, the formulation of the shear stress is given by the following equation:

$$\tau(x) = (2\alpha_1 + \frac{K_s y_1}{E_1 I_1} a^2)\frac{q}{2\xi} e^{-\xi x} + \alpha_1 q(a + x) \tag{35}$$

$$\tau(x) = (\frac{K_s}{\xi^2}\left(\frac{2(y_1 + \frac{t_2}{2})}{E_1 I_1 D'_{11} + b_2} D'_{11}\right) + \frac{K_s y_1}{E_1 I_1} a^2)\frac{q}{2\xi} e^{-\xi x} + \frac{K_s}{\xi^2}\left(\frac{(y_1 + \frac{t_2}{2})}{E_1 I_1 D'_{11} + b_2} D'_{11}\right) q(a + x) \tag{36}$$

2.4. Normal stress distribution along the FRP– concrete interface:

The normal stress in the adhesive can be expressed as follows:

$$\sigma_n(x) = K_n \Delta w(x) = K_n\left[w_2(x) - w_1(x)\right] \tag{37}$$

Where K_n the normal stiffness of the adhesive is layer per unit of length and can be deduced as follows:

$$K_n = \frac{\sigma_n(x)}{\Delta w(x)} = \frac{\sigma_n(x)}{\Delta w(x)/t_a}\left(\frac{1}{t_a}\right) = \frac{E_a}{t_a} \tag{38}$$

$w_c(x)$ and $w_p(x)$ are the vertical displacements of the member 1 and 2 respectively. By deriving Eq. (27) twice it results:

$$\frac{d^2\sigma_n(x)}{dx^2} = K_n\left[\frac{d^2 w_2(x)}{dx^2} - \frac{d^2 w_1(x)}{dx^2}\right] \tag{39}$$

By considering the relations moment curvature of the concrete beam and the reinforcement plate respectively we can write:

$$\frac{d^2 w_1(x)}{dx^2} = -\frac{M_1(x)}{E_1 I_1} \quad \text{and} \quad \frac{d^2 w_2(x)}{dx^2} = -\frac{D'_{11} M_2(x)}{E_2 I_2} \tag{40}$$

Based on the equations of balance (3) and (8), the differential equations of equilibrium of the members 1 and 2 expressed as a function of the shear stresses and the normal stresses are given as follows:

The balance of members 1 and 2 leads to the following relationships:

$$\text{Adherent1:} \quad \frac{d^4 w_1(x)}{dx^4} = \frac{1}{E_1 I_1} b_2 \sigma_n(x) + \frac{y_1}{E_1 I_1} b_2 \frac{d\tau(x)}{dx} + \frac{q}{E_1 I_1} \tag{41}$$

$$\text{Adherent 2:} \quad \frac{d^4 w_2(x)}{dx^4} = -D'_{11}\sigma_n(x) + D'_{11}\frac{t_2}{2}\frac{d\tau(x)}{dx} \tag{42}$$

The substitution of Eqs. (41) and (42) in the fourth derivative of the normal stress obtained from Eq. (37) gives the differential equation governing the normal interface stress:

$$\frac{d^4\sigma_n(x)}{dx^4} + K_n\left(D_{11}^{'} + \frac{b_2}{E_1 I_1}\right)\sigma_n(x) - K_n\left(D_{11}^{'}\frac{t_2}{2} - \frac{y_1 b_2}{E_1 I_1}\right)\frac{d\tau(x)}{dx} + \frac{qK_n}{E_1 I_1} = 0 \tag{43}$$

The general solution of the differential equation of order 4 is:

$$\sigma_n(x) = e^{-\delta x}\left[\Delta_3\cos(\delta x) + \Delta_4\sin(\delta x)\right] + e^{\delta x}\left[\Delta_5\cos(\delta x) + \Delta_6\sin(\delta x)\right] \\ - \frac{y_1 b_2 - \frac{D_{11}^{'}E_1 I_1 t_2}{2}}{D_{11}^{'}E_1 I_1 + b_2}\frac{d\tau(x)}{dx} - \frac{1}{D_{11}^{'}E_1 I_1 + b_2}q \tag{44}$$

For large values of "x" we assume that the normal stress tends to zero, and it results $\Delta_5 = \Delta_6 = 0$. The general solution becomes:

$$\sigma_n(x) = e^{-\delta x}\left[\Delta_3\cos(\delta x) + \Delta_4\sin(\delta x)\right] - \frac{y_1 b_2 - \frac{D_{11}^{'}E_1 I_1 t_2}{2}}{D_{11}^{'}E_1 I_1 + b_2}\frac{d\tau(x)}{dx} - \frac{1}{D_{11}^{'}E_1 I_1 + b_2}q \tag{45)}$$

Where

$$\delta = \sqrt[4]{\frac{K_n}{4}\left(D_{11}^{'} + \frac{b_2}{E_1 I_1}\right)} \tag{46}$$

The integration constants Δ_3 and Δ_4 are given by:

$$\Delta_3 = \frac{K_n}{2\delta^3 E_1 I_1}\left[V_T(0) + \delta M_T(0)\right] - b_2 K_n\left(\frac{y_1}{E_1 I_1} - \frac{D_{11}^{'}t_2}{2b_2}\right)\frac{\tau(0)}{2\delta^3} \\ + \frac{y_1 b_2 - \frac{D_{11}^{'}E_1 I_1 t_2}{2}}{2\delta^3(D_{11}^{'}E_1 I_1 + b_2)}\left(\frac{d^4\tau(0)}{dx^4} + \delta\frac{d^3\tau(0)}{dx^3}\right) \tag{47}$$

$$\Delta_4 = -\frac{K_n}{2\delta^2 E_1 I_1}M_T(0) - \frac{y_1 b_2 - \frac{D_{11}^{'}E_1 I_1 t_2}{2}}{2\delta^2(D_{11}^{'}E_1 I_1 + b_2)}\frac{d^3\tau(0)}{dx^3} \tag{48}$$

The above expressions for the constants Δ_3 and Δ_4 has been left in terms of the bending moment $M_T(0)$ and shear force $V_T(0)$ at the end of the soffit plate. With the constants Δ_3 and Δ_4 determined, the interfacial normal stress can then be found using Eq.(45).

3. Numerical results and discussions:

3.1 Material used:

The material used for the present studies is an RC cantilever beam bonded with different type of composite materials plate (GFRP, CFRP, Sika Carbodur, Sika Wrap and FGM). A summary of the geometric and material properties is given in Table 1 and Fig. 3. The span of the RC cantilever

Table 1 Mechanical properties of the materials used

Component	Young's modulus (MPa)	Poisson's ratio
RC cantilever beam	E_1 = 30000	0.18
Adhesive layer	E_a = 6700	0.4
Sika Carbodur strengthening plate	E_2= 165 000	0.3
Sika Wrap strengthening plate	E_2= 230 000	0.3
CFRP strengthening plate	E_2= 140 000	0.28
GFRP strengthening plate	E_2= 50 000	0.28
FGM (Al_2O_3) strengthening plate	$E_{ceramic}$ = 380 000, E_{metal}= 70 000	0.3

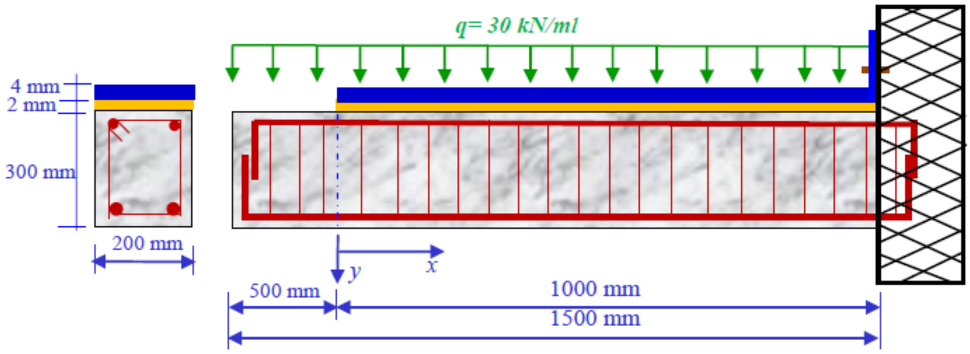

Fig. 3 Geometric characteristic of a RC cantilever member strengthening with composite plate

beam is 1500 mm, the distance from the support to the end of the plate is 500 mm and the uniformly distributed load (UDL) is 30 kN/m.

3.2 Comparison with analytical solutions

A comparison between the interfacial shear and normal stresses from the different existing closed-form solutions (Xue-jun *et al*. 2019) and the present new solution is undertaken in this section. An RC beam bonded with a CFRP soffit plate is being considered. The beam is simply supported and subjected to a uniformly distributed load. A summary of the geometric and material properties is given in Table 1 and Fig. 3. The span of The RC cantilever beam is 1500 mm, the distance from the support to the end of the plate is 300 mm and the uniformly distributed load is 30 kN/m. Fig. 4 shows the distribution of the interfacial shear stress and the longitudinal normal stress near the plate end for the example RC cantilever beam bonded with a CFRP plate for the uniformly distributed load case. It can be seen from the figure that the stress distributions predicted by the present method are in good agreement with those obtained by using other methods.

3.3 Parametric studies

The parametric study program is based on this analytical work approach, which will help engineers in optimizing their design parameters, the effects of several parameters were investigated.

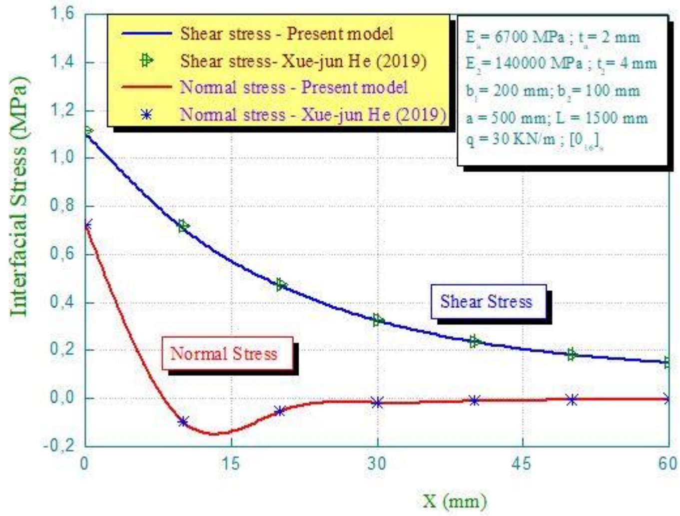

Fig. 4 Comparison of interfacial shear and normal stress for CFRP-plated RC cantilever beam with the analytical results

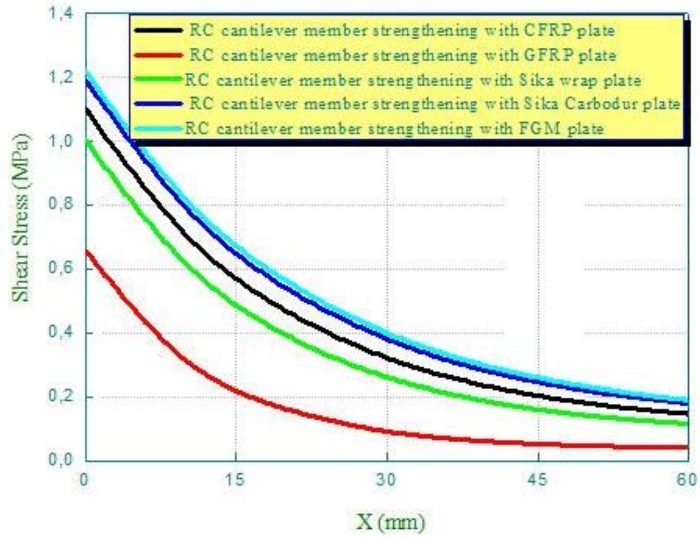

Fig. 5 Effect of plate stiffness on interfacial shear stress in strengthened RC cantilever beam

3.3.1 Effect of plate stiffness on interfacial stress

Figs. 5 and 6 gives interfacial normal and shear stresses for the RC cantilever beam bonded with a CFRP plate, GFRP plate, Sika Carbodur plate, Sika Wrap plate and FGM plate, respectively, which demonstrates the effect of plate material properties on interfacial stresses. The length of the plate is Lp=1000 mm, and the thickness of the plate and the adhesive layer are both 4 mm. The results show that, as the plate material becomes softer (from steel to CFRP and then GFRP - by decreasing order from the FGM plate to the Sika Carbodur plate, the CFRP plate, the Sika Wrap plate and to GFRP plate “the least rigid”), the interfacial stresses become smaller, as

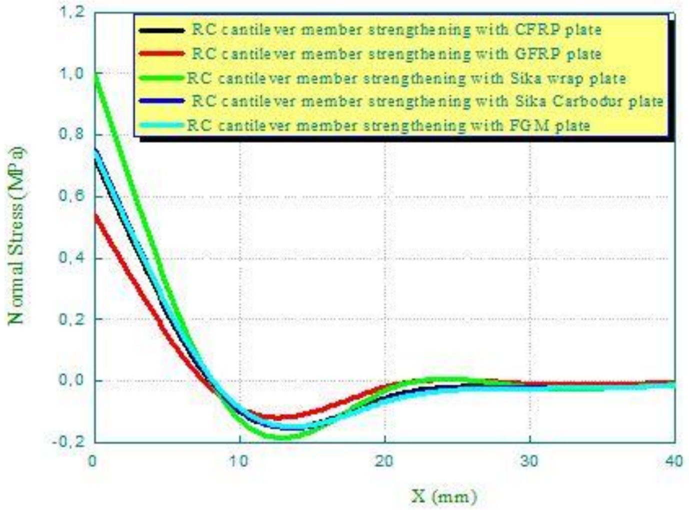

Fig. 7 Effect of length of unstrengthened on interfacial shear stress in strengthened RC cantilever beam

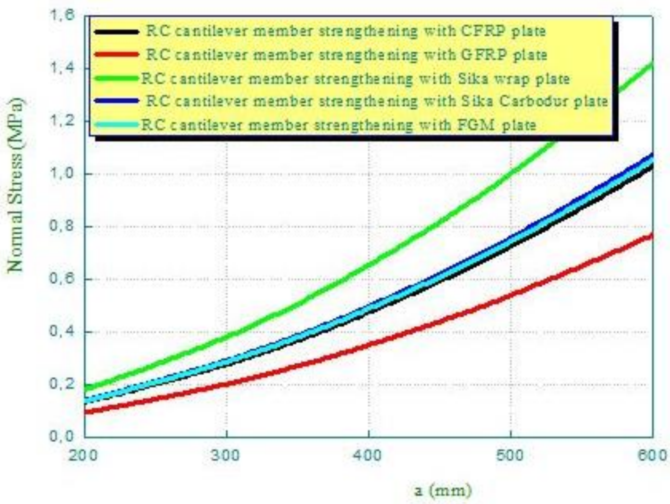

Fig. 8 Effect of length of unstrengthened on interfacial normal stress in strengthened RC cantilever beam

expected. This is because, under the same load, the tensile force developed in the plate is smaller, which leads to reduced interfacial stresses. The position of the peak interfacial shear stress moves closer to the free edge as the plate becomes less stiff.

3.3.2 Effect of length of unstrengthened region "a"

The influence of the length of the ordinary-beam region (the region between the free edge of the cantilever beam and the end of the composite strip on the edge stresses) appears in Figs. 7 and 8. It is seen that, as the plate terminates further away from the supports, the interfacial stresses

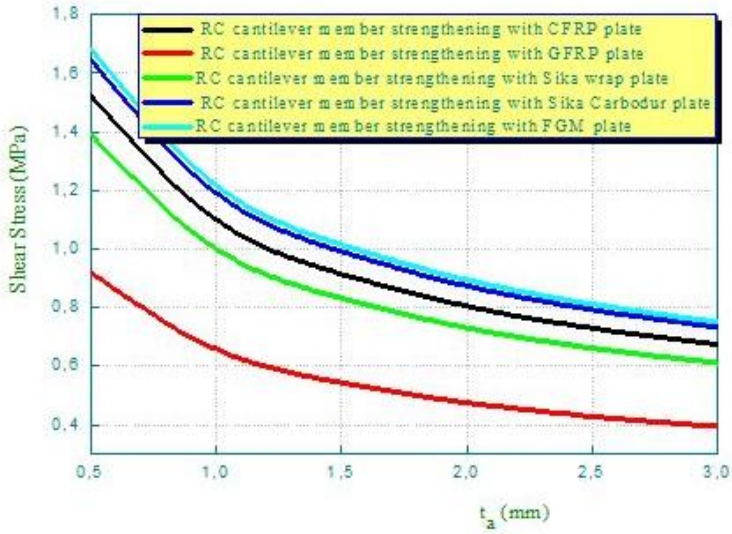

Fig. 9 Effect of the thickness of the adhesive layer on interfacial shear stress in strengthened RC cantilever beam

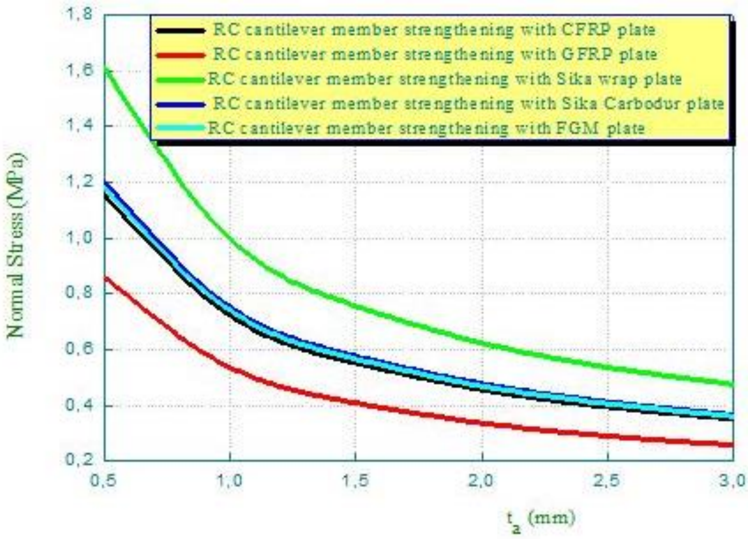

Fig. 10 Effect of the thickness of the adhesive layer on interfacial normal stress in strengthened RC cantilever beam

decrease significantly. This result reveals that in any case of strengthening, including cases where retrofitting is required in a limited zone of maximum bending moments at the level of the double support of the beam where the moment is maximum, it is recommended to extend the strengthening strip as possible to the lines, at the free end.

3.3.3 Effect of the thickness of the adhesive layer

It can be seen from Figs. 9 and 10 that the thickness of adhesive layer affects only the normal

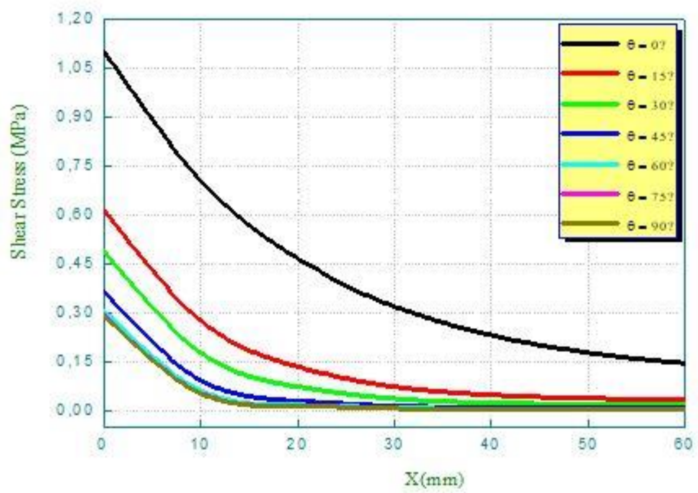

Fig. 11 Effect of fiber orientation on the CFRP plate on interfacial shear stress in strengthened RC cantilever beam

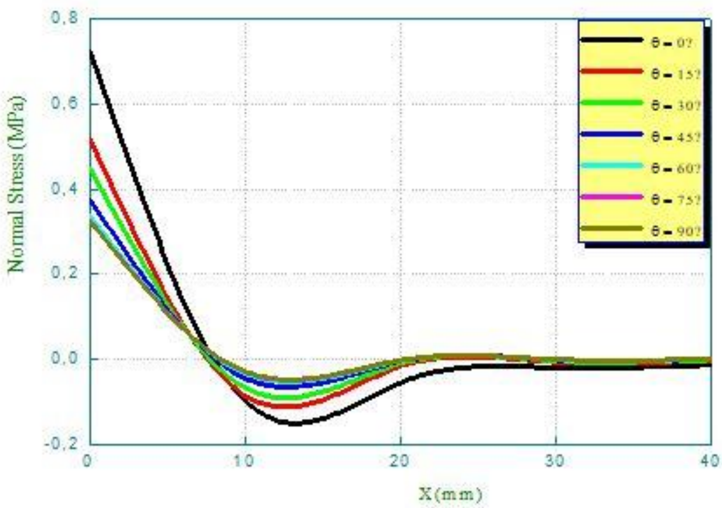

Fig. 12 Effect of fiber orientation on the CFRP plate on interfacial normal stress in strengthened RC cantilever beam

and shear stress concentrations, hardly the stress levels. However, design of the properties and thickness of the adhesive is a difficult problem. An optimization design of the adhesive is expected. As well by noting that the greater the thickness of adhesive layer becomes (increases) the more the stresses decrease, it is possible to say that the increase in thickness of adhesive layer is inversely proportional to the stresses of interfaces.

3.3.4 Effect of fiber orientation on the CFRP plate:

The effect of fiber orientation on adhesive stresses is show in Figs. 11, 12 and 13, the maximum interfacial stresses increase with increasing alignment of all high strength fibers in the composite

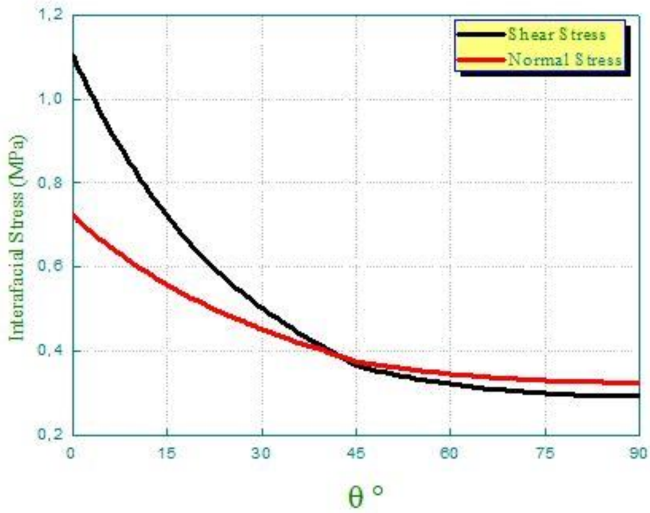

Fig. 13 Effect of fiber orientation on the CFRP plate on interfacial shear and normal stress in strengthened RC cantilever beam

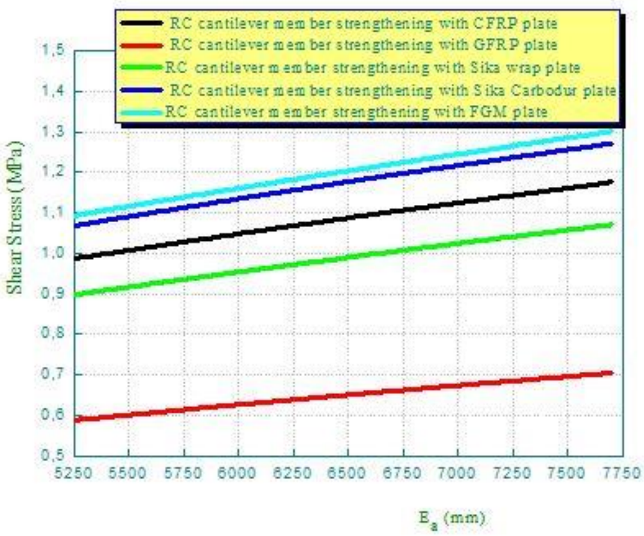

Fig. 14 Effect of the Young's modulus of the adhesive layer on interfacial shear stress in strengthened RC cantilever beam

plate in beam's longitudinal direction x.

3.3.5 Effect of elasticity modulus of adhesive layer on interfacial stress

The adhesive layer is a relatively soft, isotropic material and has a smaller stiffness. The six sets of elasticity modulus are considered here, which are 5250, 5750, 6250, 6750, 7250 and 7750 MPa. The Poisson's ratio of the adhesive is kept constant. The numerical results in Figs. 14 and 15 show that the property of the adhesive hardly influences the level of the interfacial stresses,

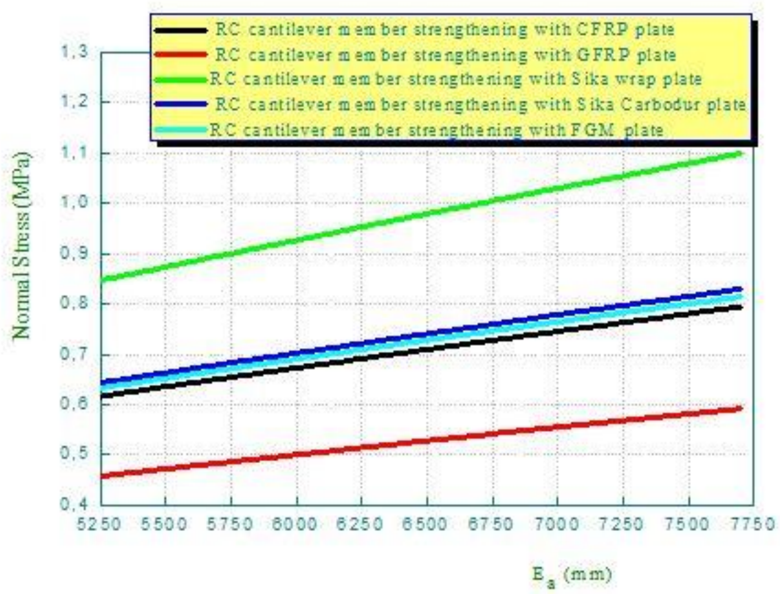

Fig. 15 Effect of the Young's modulus of the adhesive layer on interfacial normal stress in strengthened RC cantilever beam

whether normal or shear stress, but the stress concentrations at the end of the plate increase as the Young's modulus of the adhesive increases.

4. Conclusions

In this paper, analytical analysis was conducted to investigate the interfacial stresses in RC cantilever members externally bonded with a CFRP plate, GFRP plate, Sika Carbodur plate, Sika Wrap plate and FGM plate, respectively. According to the deformation compatibility and static equilibrium conditions, a linear elastic analytical model was developed under a uniformly distributed load. we recorded a good convergence of the results obtained by comparisons with those existing in the literature, it is from this comparison that we confirm the reliability of the present theory. The given expressions are simple and suitable for manually calculating the interfacial stresses and the longitudinal strain in composite of flexural composite strengthened cantilever members before the local debonding initiation occurred. From the results obtained, we have drawn a few remarks, as examples: The distributions of interfacial stresses and the stress concentrations in composite strengthened RC cantilever members are influenced by various parameters. Under the same conditions, the maximum interfacial stresses and the risk of free of composite end-debonding can be decreased to varying the stiffness of the composite, increasing composite bonding length and increasing adhesive layer thickness, and by using less rigid composite with high tensile strength. These results are useful for engineers seeking to optimize strengthening design parameters and implement reliable debonding prevention measures. Unlike to the classical solutions, the present solution is general in nature and may be applicable to all kinds of materials.

Acknowledgments

This research was supported by the Algerian Ministry of Higher Education and Scientific Research (MESRS) as part of the grant for the PRFU research project n° A01L02UN140120200002 and by the University of Tiaret, in Algeria.

References

Abdelhak, Z., Hadji, L., Daouadji, T.H. and Adda Bedia, E.A. (2016), "Thermal buckling response of functionally graded sandwich plates with clamped boundary conditions", *Smart Struct. Syst.*, **18**(2), 267-291. https://doi.org/10.12989/sss.2016.18.2.267.

Abdelouahed, T. (2006), "Improved theoretical solution for interfacial stresses in concrete beams strengthened with FRP plate", *Int. J. Solids Struct.*, **43**(14-15), 4154-4174. https://doi.org/10.1016/j.ijsolstr.2005.03.074.

Abderezak, R., Daouadji, T.H. and Rabia, B. (2020), "Analysis of interfacial stresses of the reinforced concrete foundation beams repairing with composite materials plate", *Coupled Syst. Mech.*, **9**(5), 473-498. http://dx.doi.org/10.12989/csm.2020.9.5.473.

Abderezak, R., Daouadji, T.H. and Rabia, B. (2021), "Aluminum beam reinforced by externally bonded composite materials", *Advan. Mater. Res.*, **10**(1), 23-44. http://dx.doi.org/10.12989/amr.2021.10.1.023.

Abderezak, R., Daouadji, T.H. and Rabia, B. (2021), "Aluminum beam reinforced by externally bonded composite materials", *Advan. Mater. Res.*, **10**(1), 23. http://dx.doi.org/10.12989/amr.2020.9.4.265.

Abderezak, R., Daouadji, T.H. and Rabia, B. (2021), "Modeling and analysis of the imperfect FGM-damaged RC hybrid beams", 1, 6(2), 117. http://dx.doi.org/10.12989/acd.2021.6.2.117

Abderezak, R., Daouadji, T.H., Abbes, B., Rabia, B., Belkacem, A. and Abbes, F. (2017), "Elastic analysis of interfacial stress concentrations in CFRP-RC hybrid beams: Effect of creep and shrinkage", *Advan. Mater. Res.*, **6**(3), 257. https://doi.org/10.12989/amr.2017.6.3.257.

Abderezak, R., Daouadji, T.H., Rabia, B. and Belkacem, A. (2018), "Nonlinear analysis of damaged RC beams strengthened with glass fiber reinforced polymer plate under symmetric loads", *Earthq. Struct.*, **15**(2), 113-122. https://doi.org/10.12989/eas.2018.15.2.113.

Abderezak, R., Rabia, B., Daouadji, T.H., Abbes, B., Belkacem, A. and Abbes, F. (2018), "Elastic analysis of interfacial stresses in prestressed PFGM-RC hybrid beams", *Advan. Mater. Res.*, **7**(2), 83. https://doi.org/10.12989/amr.2018.7.2.083.

Adim, B. and Daouadji, T.H. (2016), "Effects of thickness stretching in FGM plates using a quasi-3D higher order shear deformation theory", *Advan. Mater. Res.*, **5**(4), 223. https://doi.org/10.12989/amr.2016.5.4.223.

Adim, B., Daouadji, T.H. and Abbes, B. (2016), "Buckling analysis of anti-symmetric cross-ply laminated composite plates under different boundary conditions", *Int. Appl. Mech.*, **52**(6), 661-676. https://doi.org/10.1007/s10778-016-0787-x

Adim, B., Daouadji, T.H., Abbes, B. and Rabahi, A. (2016), "Buckling and free vibration analysis of laminated composite plates using an efficient and simple higher order shear deformation theory", *Mech. Ind.*, **17**(5), 512. https://doi.org/10.1051/meca/2015112.

Adim, B., Daouadji, T.H., Rabia, B. and Hadji, L. (2016), "An efficient and simple higher order shear deformation theory for bending analysis of composite plates under various boundary conditions", *Earthq. Struct.*, **11**(1), 63-82. https://doi.org/10.12989/eas.2016.11.1.063.

Aicha, K., Rabia, B., Daouadji, T.H. and Bouzidene, A. (2020), "Effect of porosity distribution rate for bending analysis of imperfect FGM plates resting on Winkler-Pasternak foundations under various boundary conditions", *Coupled Syst. Mech.*, **9**(6), 575-597. http://dx.doi.org/10.12989/csm.2020.9.6.575.

Alam, M.A. and Al Riyami, K. (2018), "Shear strengthening of reinforced concrete beam using natural fibre reinforced polymer laminates", *Construct. Build. Mater.*, **162**, 683-696.

https://doi.org/10.1016/j.conbuildmat.2017.12.011.

AlSaid-Alwan, H.H.S. and Avcar, M. (2020), "Analytical solution of free vibration of FG beam utilizing different types of beam theories: A comparative study", *Comput. Concrete*, **26**(3), 285-292. http://dx.doi.org/10.12989/cac.2020.26.3.285.

Batou, B., Nebab, M., Bennai, R., Atmane, H.A., Tounsi, A. and Bouremana, M. (2019), "Wave dispersion properties in imperfect sigmoid plates using various HSDTs", *Steel Compos. Struct.*, **33**(5), 699-716. https://doi.org/10.12989/scs.2019.33.5.699.

Belkacem, A., Tahar, H.D., Abderrezak, R., Amine, B.M., Mohamed, Z. and Boussad, A. (2018), "Mechanical buckling analysis of hybrid laminated composite plates under different boundary conditions", *Struct. Eng. Mech*., **66**(6), 761-769. https://doi.org/10.12989/sem.2018.66.6.761.

Bendada, A., Boutchicha, D., Khatir, S., Magagnini, E., Capozucca, R. and Abdel Wahab, M. (2020), "Mechanical characterization of an epoxy panel reinforced by date palm petiole particle", *Steel Compos. Struct*., **35**(5), 627-634. https://doi.org/10.12989/scs.2020.35.5.627.

Benferhat, R., Daouadji, T.H. and Mansour, M.S. (2016), "Free vibration analysis of FG plates resting on an elastic foundation and based on the neutral surface concept using higher-order shear deformation theory", *Comptes Rendus Mecanique*, **344**(9), 631-641. https://doi.org/10.1016/j.crme.2016.03.002.

Benferhat, R., Daouadji, T.H., Mansour, M.S. and Hadji, L. (2016), "Effect of porosity on the bending and free vibration response of functionally graded plates resting on Winkler-Pasternak foundations", *Earthq. Struct*., **10**(6), 1429-1449. https://doi.org/10.12989/eas.2016.10.6.1429.

Benferhat, R., Hassaine Daouadji, T. and Rabahi, A. (2021a), "Effect of porosity on fundamental frequencies of FGM sandwich plates", *Compos. Mater. Eng*., **3**(1), 25-40. http://dx.doi.org/10.12989/cme.2021.3.1.025.

Benferhat, R., Hassaine Daouadji, T. and Rabahi, A. (2021b), "Effect of air bubbles in concrete on the mechanical behavior of RC beams strengthened in flexion by externally bonded FRP plates under uniformly distributed loading", *Compos. Mater. Eng*., **3**(1), 41-55. http://dx.doi.org/ 10.12989/cme.2021.3.1.041.

Benhenni, M.A., Daouadji, T.H., Abbes, B., Abbes, F., Li, Y. and Adim, B. (2019), "Numerical analysis for free vibration of hybrid laminated composite plates for different boundary conditions", *Struct. Eng. Mech*., **70**(5), 535-549. https://doi.org/10.12989/sem.2019.70.5.535.

Benhenni, M.A., Daouadji, T.H., Abbes, B., Adim, B., Li, Y. and Abbes, F. (2018), "Dynamic analysis for anti-symmetric cross-ply and angle-ply laminates for simply supported thick hybrid rectangular plates", *Advan. Mater. Res*., **7**(2), 119. https://doi.org/10.12989/amr.2018.7.2.119.

Bensattalah, T., Daouadji, T.H. and Zidour, M. (2019), "Influences the Shape of the Floor on the Behavior of Buildings Under Seismic Effect", *In International Symposium on Materials and Sustainable Development*, Springer, Cham. https://doi.org/10.1007/978-3-030-43268-3_3.

Bensattalah, T., Zidour, M. and Daouadji, T.H. (2018), "Analytical analysis for the forced vibration of CNT surrounding elastic medium including thermal effect using nonlocal Euler-Bernoulli theory", *Advan. Mater. Res.*, **7**(3), 163-174. https://doi.org/10.12989/amr.2018.7.3.163.

Benyoucef, S., Tounsi, A., Meftah, S.A. and Adda-Bedia, E.A. (2006), "Approximate analysis of the interfacial stress concentrations in FRP–RC hybrid beams", *Compos. Interf*., **13**(7), 561-571. https://doi.org/10.1163/156855406778440758.

Chedad, A., Daouadji, T.H., Abderezak, R., Belkacem, A., Abbes, B., Rabia, B. and Abbes, F. (2017), "A high-order closed-form solution for interfacial stresses in externally sandwich FGM plated RC beams", *Advan. Mater. Res*., **6**(4), 317. https://doi.org/10.12989/amr.2017.6.4.317.

Chergui, S., Daouadji, T.H., Hamrat, M., Boulekbache, B., Bougara, A., Abbes, B. and Amziane, S. (2019), "Interfacial stresses in damaged RC beams strengthened by externally bonded prestressed GFRP laminate plate: Analytical and numerical study", *Advan. Mater. Res*., **8**(3), 197-217. https://doi.org/10.12989/amr.2019.8.3.197.

Daouadji, H.T., Benyoucef, S., Tounsi, A., Benrahou, K.H. and Bedia, A.E. (2008), "Interfacial stress concentrations in FRP-damaged RC hybrid beams", *Compos. Interfaces*, **15**(4), 425-440. https://doi.org/10.1163/156855408784514702.

Daouadji, T.H. (2013), “Analytical analysis of the interfacial stress in damaged reinforced concrete beams strengthened by bonded composite plates”, *Strength Mater*., **45**(5), 587-597. https://doi.org/10.1007/s11223-013-9496-4.

Daouadji, T.H. (2017), “Analytical and numerical modeling of interfacial stresses in beams bonded with a thin plate”, *Advan. Comput. Design*, **2**(1), 57-69. https://doi.org/10.12989/acd.2017.2.1.057.

Daouadji, T.H., Chedad, A. and Adim, B. (2016), “Interfacial stresses in RC beam bonded with a functionally graded material plate”, *Struct. Eng. Mech*., **60**(4), 693-705. http://dx.doi.org/10.12989/sem.2016.60.4.693.

Daouadji, T.H., Rabahi, A., Abbes, B. and Adim, B. (2016), “Theoretical and finite element studies of interfacial stresses in reinforced concrete beams strengthened by externally FRP laminates plate”, *J. Adhesion Sci. Technol*., **30**(12), 1253-1280. https://doi.org/10.1080/01694243.2016.1140703.

Guenaneche, B. and Tounsi, A. (2014), “Effect of shear deformation on interfacial stress analysis in plated beams under arbitrary loading”, *Int. J. Adhesion Adhesives*, **48**, 1-13. https://doi.org/10.1016/j.ijadhadh.2013.09.016.

Hadj, B., Rabia, B. and Daouadji, T.H. (2019), “Influence of the distribution shape of porosity on the bending FGM new plate model resting on elastic foundations”, *Struct. Eng. Mech*., **72**(1), 61-70. https://doi.org/10.12989/sem.2019.72.1.061.

Hadj, B., Rabia, B. and Daouadji, T.H. (2021), “Vibration analysis of porous FGM plate resting on elastic foundations: effect of the distribution shape of porosity”, *Coupled Syst. Mech*., **10**(1), 61-77 http://dx.doi.org/10.12989/csm.2021.10.1.061

Hamrat, M., Bouziadi, F., Boulekbache, B., Daouadji, T.H., Chergui, S., Labed, A. and Amziane, S. (2020), “Experimental and numerical investigation on the deflection behavior of pre-cracked and repaired reinforced concrete beams with fiber-reinforced polymer”, *Construct. Build. Mater*., **249**, 118745. http://dx.doi.org/10.1016/j.conbuildmat.2020.118745.

He, X.J., Zhou, C.Y. and Wang, Y. (2020), “Interfacial stresses in reinforced concrete cantilever members strengthened with fibre-reinforced polymer laminates”, *Advan. Struct. Eng*., **23**(2), 277-288. https://doi.org/10.1177/1369433219868933.

Krour, B., Bernard, F. and Tounsi, A. (2013), “Fibers orientation optimization for concrete beam strengthened with a CFRP bonded plate: A coupled analytical–numerical investigation”, *Eng. Struct*., **56**, 218-227. https://doi.org/10.1016/j.engstruct.2013.05.008.

Larrinaga, P., Garmendia, L., Piñero, I. and San-José, J.T. (2020), “Flexural strengthening of low-grade reinforced concrete beams with compatible composite material: Steel Reinforced Grout (SRG)”, *Construct. Build. Mater*., **235**, 117790. https://doi.org/10.1016/j.conbuildmat.2019.117790.

Liu, S., Zhou, Y., Zheng, Q., Zhou, J., Jin, F. and Fan, H. (2019), “Blast responses of concrete beams reinforced with steel-GFRP composite bars”, *In Structures*, Elsevier. https://doi.org/10.1016/j.istruc.2019.08.010.

Mahi, B.E., Benrahou, K.H., Belakhdar, K., Tounsi, A. and Bedia, E.A. (2014), “Effect of the tapered end of a FRP plate on the interfacial stresses in a strengthened beam used in civil engineering applications”, *Mech. Compos. Mater*., **50**(4), 467-476. https://doi.org/10.1007/s11029-014-9433-z.

Panjehpour, M., Ali, A.A.A., Voo, Y.L. and Aznieta, F.N. (2014), “Effective compressive strength of strut in CFRP-strengthened reinforced concrete deep beams following ACI 318-11”, *Comput. Concrete*, **13**(1), 135-147. https://doi.org/10.12989/cac.2014.13.1.135.

Panjehpour, M., Farzadnia, N., Demirboga, R. and Ali, A.A.A. (2016), “Behavior of high-strength concrete cylinders repaired with CFRP sheets”, *J. Civil Eng. Manage*., **22**(1), 56-64. https://doi.org/10.3846/13923730.2014.897965.

Rabahi, A., Daouadji, T.H., Abbes, B. and Adim, B. (2016), “Analytical and numerical solution of the interfacial stress in reinforced-concrete beams reinforced with bonded prestressed composite plate”, *J. Reinforce. Plastics Compos*., **35**(3), 258-272. https://doi.org/10.1177/0731684415613633.

Rabia, B., Abderezak, R., Daouadji, T.H., Abbes, B., Belkacem, A. and Abbes, F. (2018), “Analytical analysis of the interfacial shear stress in RC beams strengthened with prestressed exponentially-varying properties plate”, *Advan. Mater. Res*., **7**(1), 29. https://doi.org/10.12989/amr.2018.7.1.029.

Rabia, B., Daouadji, T. H. and Abderezak, R. (2019), “Effect of porosity in interfacial stress analysis of perfect FGM beams reinforced with a porous functionally graded materials plate”, *Struct. Eng. Mech*., **72**(3), 293-304. https://doi.org/10.12989/sem.2019.72.3.293.

Rabia, B., Daouadji, T.H. and Abderezak, R. (2019), “Effect of distribution shape of the porosity on the interfacial stresses of the FGM beam strengthened with FRP plate”, *Earthq. Struct*., **16**(5), 601-609. https://doi.org/10.12989/eas.2019.16.5.601

Rabia, B., Tahar, H.D. and Abderezak, R. (2020), “Thermo-mechanical behavior of porous FG plate resting on the Winkler-Pasternak foundation”, *Coupled. Syst. Mech*., **9**(6), 499-519. http://dx.doi.org/10.12989/csm.2020.9.6.499.

Salah, F., Boucham, B., Bourada, F., Benzair, A., Bousahla, A.A. and Tounsi, A. (2019), “Investigation of thermal buckling properties of ceramic-metal FGM sandwich plates using 2D integral plate model”, *Steel Compos. Struct*., **33**(6), 805-822. https://doi.org/10.12989/scs.2019.33.6.805.

Smith, S.T. and Teng, J.G. (2001), “Interfacial stresses in plated beams”, *Eng. Struct*., **23**(7), 857-871. http://dx.doi.org/10.1016/S0141-0296(00)00090-0.

Tahar, H.D., Abderezak, R. and Rabia, B. (2020), “Flexural performance of wooden beams strengthened by composite plate”, *Struct. Monit. Maintain*, **7**(3), 233-259. http://dx.doi.org/10.12989/smm.2020.7.3.233.

Tahar, H.D., Boussad, A., Abderezak, R., Rabia, B., Fazilay, A. and Belkacem, A. (2019), “Flexural behaviour of steel beams reinforced by carbon fibre reinforced polymer: Experimental and numerical study”, *Struct. Eng. Mech*., **72**(4), 409-420. https://doi.org/10.12989/sem.2019.72.4.409.

Tahar, H.D., Tayeb, B., Abderezak, R. and Tounsi, A. (2021), “New approach of composite wooden beam-reinforced concrete slab strengthened by external bonding of prestressed composite plate: Analysis and modeling”, *Struct. Eng. Mech*., **78**(3), 319-332. http://dx.doi.org/10.12989/sem.2021.78.3.31.

Tayeb, B. and Daouadji, T.H. (2020), “Improved analytical solution for slip and interfacial stress in composite steel-concrete beam bonded with an adhesive”, *Advan. Mater. Res*., **9**(2), 133-153. https://doi.org/10.12989/amr.2020.9.2.133.

Tlidji, Y., Benferhat, R. and Tahar, H.D. (2021), “Study and analysis of the free vibration for FGM microbeam containing various distribution shape of porosity”, *Struct. Eng. Mech*., **77**(2), 217. http://dx.doi.org/10.12989/sem.2021.77.2.217.

Tounsi, A., Daouadji, T.H. and Benyoucef, S. (2009), “Interfacial stresses in FRP-plated RC beams: Effect of adherend shear deformations”, *Int. J. Adhesion Adhesives*, **29**(4), 343-351. https://doi.org/10.1016/j.ijadhadh.2008.06.008.

Wang, Y.H., Yu, J., Liu, J.P., Zhou, B.X. and Chen, Y.F. (2020), “Experimental study on assembled monolithic steel-prestressed concrete composite beam in negative moment”, *J. Construct. Steel Res*., **167**, 105667. https://doi.org/10.1016/j.jcsr.2019.06.004.

Yang, J. and Wu, Y.F. (2007), “Interfacial stresses of FRP strengthened concrete beams: Effect of shear deformation.”, *Compos. Struct*., **80**(3), 343-351. https://doi.org/10.1016/j.compstruct.2006.05.016.

Yaylaci, M. and Avcar, M. (2020), “Finite element modeling of contact between an elastic layer and two elastic quarter planes”, *Comput. Concrete*, **26**(2), 107-114. http://dx.doi.org/10.12989/cac.2020.26.2.107.

Yuan, C., Chen, W., Pham, T.M. and Hao, H. (2019), “Effect of aggregate size on bond behaviour between basalt fibre reinforced polymer sheets and concrete”, *Compos. Part B: Eng*., **158**, 459-474. https://doi.org/10.1016/j.compositesb.2018.09.089.

Zenzen, R., Khatir, S., Belaidi, I., Le Thanh, C. and Wahab, M.A. (2020), “A modified transmissibility indicator and Artificial Neural Network for damage identification and quantification in laminated composite structures”, *Compos. Struct*., **248**, 112497. https://doi.org/10.1016/j.compstruct.2020.112497.

Zohra, A., Benferhat, R., Tahar, H.D. and Tounsi, A. (2021), “Analysis on the buckling of imperfect functionally graded sandwich plates using new modified power-law formulations”, *Struct. Eng. Mech*., **77**(6), 797-807. http://dx.doi.org/10.12989/sem.2021.77.6.797.

TK